Variable speed micro-hydro power generation system: Review and Experimental results

Baoling Guo, Seddik Bacha, Mazen Alamir, Amgad Tarek Mohamed

Variable speed micro-hydro power generation system: Review and Experimental results *

Baoling GUO[1], Seddik BACHA[1], Mazen ALAMIR[2], Amgad MOHAMED[2]

[1]Univ. Grenoble Alpes, CNRS, Grenoble INP*, G2elab, F-38000 Grenoble, France.

[2]Univ. Grenoble Alpes, CNRS, Grenoble INP*, GIPSA-Lab, F-38400 Saint Martin D'Hères, France.

ABSTRACT – Micro-hydro power has a large potential in the renewable energy context. Variable speed technique is preferable to improve the hydraulic power profitability and optimise the hydraulic transient process. First, a review of hydraulic modelling approaches is addressed. In particular, an improved hydraulic modelling approach based on the 'Hill charts' measurements is presented. Furthermore, representative power topologies employed to variable speed micro-hydro power generation systems are reviewed. A direct drive permanent magnet synchronous generator topology is implemented in this paper. Experiments are provided to verify effectiveness of the hydraulic model built and its control algorithms. Conclusions are indicated in the end.

Key words – Micro-hydro power, variable speed operation, modelling, topology, 'Hill charts', dynamics.

1. INTRODUCTION

Micro-hydro power is widely used in the renewable energy context [1]-[28]. Large applications to Micro-Hydro Power Plants (MHPPs) have proved that variable speed operations can gain more hydraulic power than the fixed speed case [1, 2, 3, 9, 17, 14]. Besides, variable speed techniques can improve the operation process such as mitigating the cavitation effects, alleviating water hammer disturbances, and optimizing transient processes [2, 3]. Due to the benefits of variable speed operation, large efforts have been contributed.

Firstly, a practical hydraulic model is the key for control law test. However, unlike the well-developed case of wind turbines which has an optimal tip speed ratio to realize the maximum power efficiency, there is no general efficiency expression for hydraulic turbines [15, 17]. The efficiency highly depends on both the geometry turbine design and its operating conditions, which are complex to be determined, numerous types of models are proposed in previous works. Some modelling approaches neglect the water flow rates variations caused by rotation speed changes [1, 9, 17]. The application scope of [1, 6, 9, 17] is limited to particular hydraulic turbines. Some dynamic models can achieve more precise curves but not practical for variable speed implementations [7, 18, 19, 25]. Considering these drawbacks, an improved modelling approach based on static measurements is proposed in [14], which could be applied to a class of micro-hydro turbines with 'Hill Chart' efficiency characteristics. Therefore, a 'Hill charts' based model is used to achieve the real-time simulation study in this paper.

Furthermore, to achieve the efficient variable speed operation, various hydraulic energy conversion topologies based on Power Electronics (PE) are proposed in [3, 4, 8, 22]. The topologies are different from several aspects : namely, generation units, mechanical coupling system, and PE connection. A review on available topologies is needed, which could help designers to make the right option.

This paper is organised as follows. Firstly, different modelling approaches applied to MHPPs are reviewed in Section 2. In particular, a modelling method based on the 'Hill Charts' measurements is described. Then, it is continued by a review on available energy conversion topologies in Section 3. The employed grid-connected architecture of a variable speed micro-power generation system and its global control design are also presented. Further more, experiments of variable speed operation and grid integration control are validated in a Power Hardware-In-the-Loop (PHIL) experiment benchmark in Section 4. Conclusions are indicated in the last section.

2. MICRO-HYDRAULIC TURBINE MODELLING

In this section, various hydraulic models are reviewed, the strengths and drawbacks of those models are remarked. Moreover, an improved modelling approach based on the so called 'Hill charts' is presented.

2.1. Hydraulic turbines

The hydraulic turbines can be classified into impulse turbine and reaction turbine as shown in Fig. 1. In fact, a large majority of MHPPs are based on "Run-of-river", which has a low head and high water flow rates [1, 2, 17, 24]. Therefore, a class of axial Micro-Hydraulic Turbines (MHTs) such as Kaplan [1], Semi-Kaplan[2, 3], Bulb [9], or Propeller [7, 17] turbines and Cross flow turbines [27] become the most attractive prime movers because of their high efficiency under such conditions.

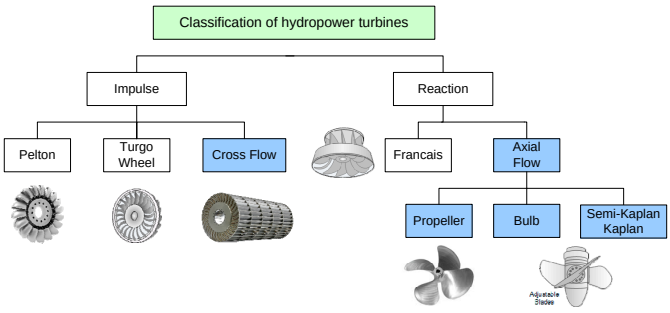

Fig. 1. Classification of hydraulic turbines

The power absorbed from the hydraulic turbine depends on the net water head $H(m)$ and the water flow rate Q_w (m^3/s) :

$$P_h = \rho \cdot g \cdot H \cdot Q_w \tag{1}$$

Hydraulic turbine efficiency η is defined as the ratio of mechanical power transmitted by the shaft to the absorbed hydraulic power, which strongly affects the net output mechanical power $P_m(watts)$:

*This paper is supported by PSPC Innov'hydro project, which specifically brings together GE Renewable, EDF (Electricity of France), Grenoble INP and other key players in the hydroelectric sector, in France

$$P_m = \eta \cdot \rho \cdot g \cdot H \cdot Q_w \tag{2}$$

where $\rho\ (kg/m^3)$ the volume density of water, g the acceleration due to gravity (m/s^2).

The mechanical torque could be given by

$$T_m = \frac{P_m}{\omega} \tag{3}$$

where $\omega\ (rad/s)$ represents the turbine rotation speed.

2.2. *Modelling approaches review*

2.2.1. *Simplified linear torque model*

A Kaplan turbine submitted to fixed head is described in [1], which has neither blade pitch control nor guide vane regulation. The hydraulic behaviour is described by a linear decreasing turbine torque (T_m) versus speed (ω) characteristic by

$$T_m = T_n(1.8 - \frac{\omega}{\omega_n}) \tag{4}$$

where T_n and ω_n represent the rated values.

This hydraulic behaviour for a fixed flow rate is presented in Fig. 2. It indicates that the torque becomes null for a rotating speed value ω_e, which is called the runaway speed. The mechanical power is consequently a parabola.

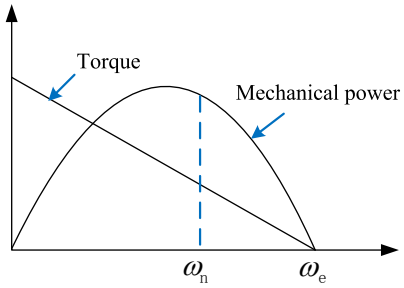

Fig. 2. Simplified linear torque model [1]

However, the turbine used in [1] includes neither blade pitch nor guide vane. Also, this paper assumes that water flow variations are very slow compared to the drive dynamics, the model in Fig. 2 only works under fixed flow rates conditions.

2.2.2. *2-D efficiency model*

In [17], a Propeller type turbine modified from a Kaplan turbine has been modelled, numerical approximations are developed to calculate hydraulic turbine efficiency. The efficiency expression is described by

$$\eta(\lambda, Q_w) = \frac{1}{2}[(\frac{90}{\lambda_i} + Q_w + 0.78)exp(\frac{-50}{\lambda_i})]3.33Q_w \tag{5}$$

$$\lambda_i = [\frac{1}{\lambda + 0.089} - 0.035]^{-1} \tag{6}$$

where $\lambda = RA\omega/Q_w$, $R\ (m)$ is the radius of the hydraulic turbine, $A\ (m^2)$ is the area swept by rotor blades, and ω (rad/s) is the hydraulic turbine rotational speed.

The efficiency curves are presented in Fig. 3. It can be observed that there always exists an optimal rotation speed to achieve the maximum efficiency under each water flow rate.

In another work [9], based on some loss curves, the efficiency η of a Bulb type turbine is modelled by

$$\eta = 1 - |\omega_{11} - Q_{11}|^{1.25} \tag{7}$$

where the turbine rotation speed ω_{11} and the discharge of water Q_{11} are both expressed in unitary values.

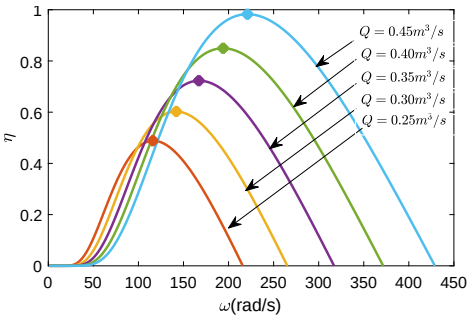

Fig. 3. 2-D efficiency model [17]

The efficiency will vary under different operation conditions. The expression indicates that only when the unitary values of rotation speed and water flow rate are the same, the efficiency is maximized, namely to be 1.

These kinds of models are improved to be suitable for varying discharge conditions. According to [10], the flow rate can be increasing or decreasing as a function of the rotational speed, depending on the specific speed and the geometrical design parameters of the turbine, for both. While these 2-D models neglect the water flow rate variations caused by rotation speed changes. Also, they are only suitable for a hydraulic turbine of neither blade pitch control nor valve regulation.

2.2.3. *Look-up table based model*

In [23], the look-up table is filled in by using a trained neural network. In order to fill in the statistic hydraulic lookup tables, it sweeps different combinations of different river flow and guide vanes position for constant water level, then the measurements under steady state are stored in the tables as shown in Fig. 4.

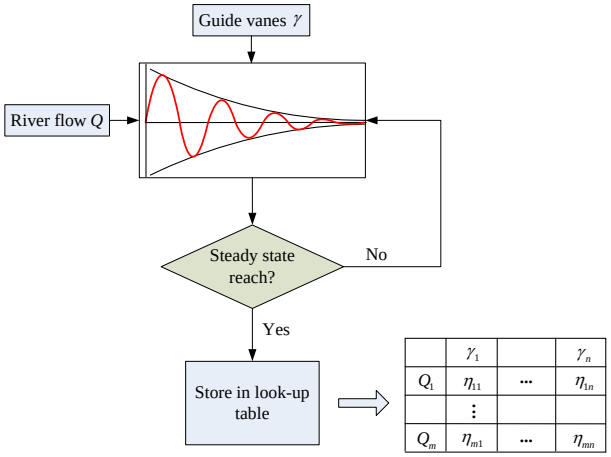

Fig. 4. Fill in the look-up table [23]

Maximum efficiency point tracking is discussed in [5]. The implemented turbine model is based on two look-up tables as illustrated in Fig. 5, where the angular position of the fixed and the rotating vanes (α and β), and the rotational speed $n(r/min)$ are considered. These tables provide the efficiency η_T and the discharge of the hydraulic turbine Q, respectively. The look-up tables have been obtained from experimental measurements carried out on a small hydro power plant.

The measured look-up table can provide a more complete model, more natural factors are considered including discharge of hydraulic turbine, guide vane opening, and pitch angle. However, a look-up table based model is not discontinuous. Besides, it is difficult to scale the obtained model to the laboratory level, consequently, the look-up tables have to be measured under a similar level MHPP.

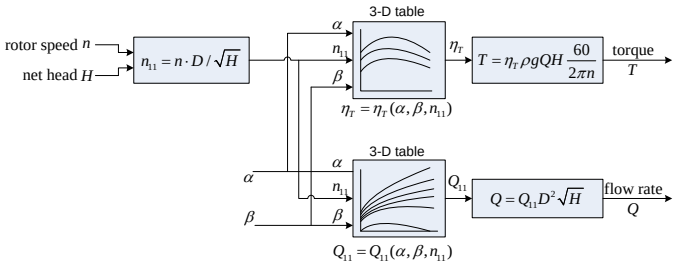

Fig. 5. Look-up table based modelling [5]

2.2.4. *Real-time efficiency model*

The efficiency is calculated in real-time in [7] by

$$\eta = \frac{P_{out}}{9.81 \cdot Q_{est} \cdot H} \tag{8}$$

The active output power P_{out} is easy to be measured. Therefore, precise estimation Q_{est} for water flow rates becomes the key for its successful application. An accurate measurement of the flow rate in low head schemes is still challenging as shown in Fig. 6. The neural-network-based estimator is used to solve the troublesome measurement of the turbine discharge in [7]. Compared with a look-up table based model, it achieves more accurate and smoother efficiency curve. However, the estimating method is very complicated for a real-time implementation.

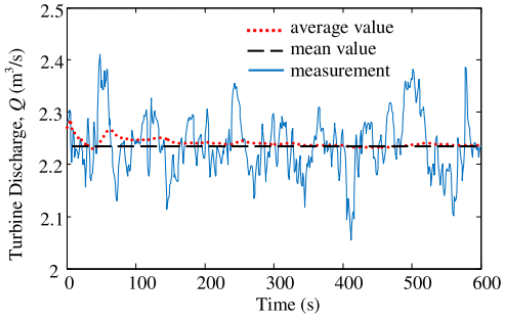

Fig. 6. Water flow measurement in a pipe [7]

2.2.5. *Dynamic hydraulic model*

A complete model of micro-hydro plant contains many modelling like penstock, wicket gate, hydraulics behaviour, and mechanical connection as shown in Fig. 8. Dynamic models are frequently discussed in the hydraulic research field [11, 16, 18, 25]. A complete control design considering large non-linear hydraulic dynamics are presented in Fig. 8. The dynamic models can be divided into linear and non-linear models as shown in Fig. 11, this classification is based on the complexity of the modelling [16]. The choosing rules of these turbine models depends on different control objectives.

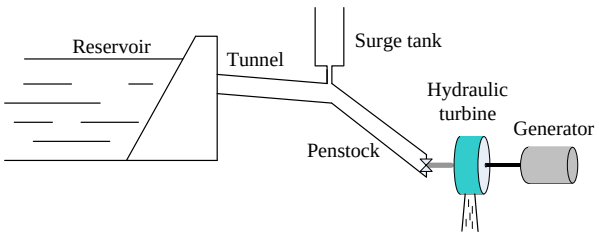

Fig. 7. Schematic of a hydro power plant

Generally, these complicated dynamic models are used in the hydraulic dynamics control study or transient process test [18],

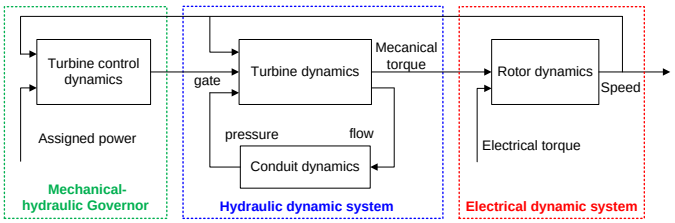

Fig. 8. Dynamic model of micro-hydraulic turbine [18]

they are studied mostly under the off-line simulation environment. But the computation burden of these non-linear dynamic models makes it too heavy to achieve real-time simulation experiments in laboratory. Also, increasing the calculation burden would deteriorate the control system behaviour. In fact, the transient hydraulic process are much longer in terms of the electrical control, therefore, the dynamics of penstock could be neglected if the implementation is dedicated to electrical control algorithms validation.

2.2.6. *Regression model*

Regression methods have been widely applied to obtain the hydraulic models. In [6], the hydraulic turbine torque is expressed by a function of speed $n(r/min)$ for different values of the guide vanes angle α as (9) presented in Fig. 9. The hydraulic behaviour is approximated by (10) shown in Fig. 10.

$$T_m^r = -1.2 \cdot n^r \cdot H^r \cdot (0.237 \cdot \alpha^{0.544}) \tag{9}$$

$$Q = 0.0166 \cdot \alpha \cdot n^r \tag{10}$$

where $T_m^r = T_t / T_{tN}$ relative torque, $n^r = n/n_N$ relative speed, $H^r = H/H_N$ relative head, $Q^r = Q/Q_N$ relative flow rate, index $'N'$ represents nominal value.

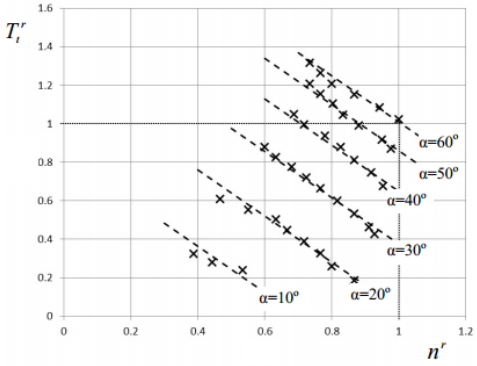

Fig. 9. Turbine torque characteristics [6]

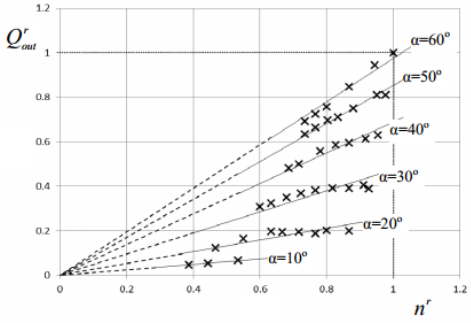

Fig. 10. Turbine flow in relation to speed [6]

In another case [15], the obtained experimental power curve has a similar shape with the parabola, Matlab function 'polyfit'

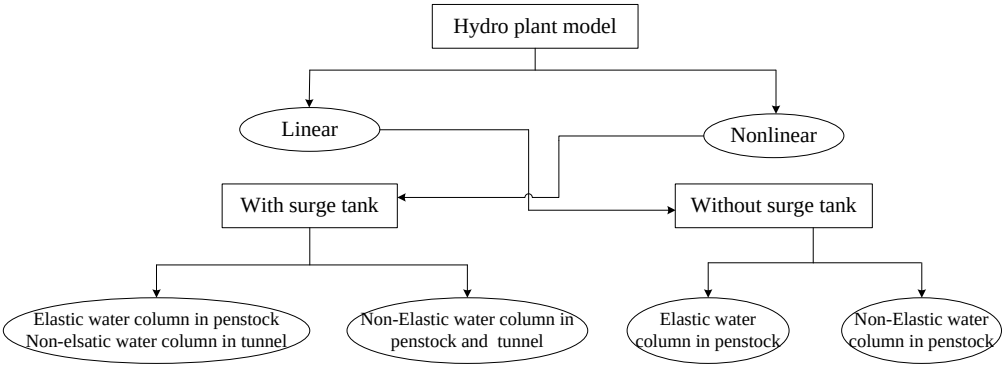

Fig. 11. Overview of hydropower plant models [16]

was used to regress power-speed relationship. The power is expressed by the rotation speed in a quadratic equation by (11). The torque could be computed according to the equation (3).

$$P_m = -1.23\omega^2 + 223.1\omega - 2623.2 \tag{11}$$

The hydraulic features in [6] are considered to be proportional to the turbine speed for a given guide vanes angle (see Fig. 10), however, according to [10], the flow rate can be increasing or decreasing with speed increasing. To simplify the modelling, the model used in [15] neglects a factor of varying water flow rates. These models still have a limitation for its applications. But the regression method is still an efficient way to obtain the hydraulic mathematical model. The key in a successful implementation is how to make use of the obtained data.

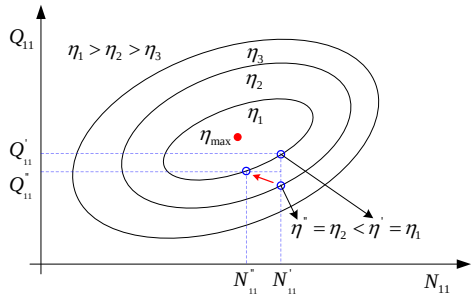

Fig. 12. 'Hill Chart' diagram and the variable speed operation, N_{11} and Q_{11} represents unit values of the turbine rotation speed and flow rates, η is the hydraulic efficiency.

Conventionally, a class of hydraulic turbines make use of the so called 'Hill Charts' (see Fig. 12) to describe the steady-state relationships among the rotational velocity $N(rpm)$, if exists the guide vanes opening $\gamma(ratio)$, the pressure head $H(m)$, the volumetric flow rate $Q(m^3/sec)$ and the turbine's mechanical torque $T(N.m)$. The 'Hill Chart' is used to determine the maximum efficiency operating point in [11, 26]. From the control viewpoint, however, it is difficult to extract a useful model from these curves [2]. Based on 'Hill charts' measurements, a regression method is proposed to obtain a 3-D hydraulic mathematical model in [14], it is well employed into Maximum Power Point Tracking (MPPT) and variable speed control. Because a systematic modelling procedure has been detailed in [14], main steps are briefly reviewed here.

2.3. 'Hill Charts' based hydraulic modelling

Due to the unavailability of micro-turbine's 'Hill Charts' data, we made use of GE's provided 'Hill Charts' of a Francis turbine which after processing, according to General Electric (GE) engineers, could be down-scaled to approximate the behaviour of a micro-turbine, for example tuning the data points using the new turbine's diameter D, maximum values of $(N, \gamma, H, Q,$ and $T)$, in addition, the unstable region (S-region) of the 'Hill Charts' of the Francis turbine can be removed which helps in smoothing the 'Hill Charts' to facilitate the model generation.

2.3.1. Model generation

The 'Hill charts' are generally represented using unitary variables N_{11}, Q_{11} and T_{11} for each γ opening, where :

$$N_{11} = \frac{ND}{\sqrt{H}} \; ; \; Q_{11} = \frac{Q}{D^2\sqrt{H}} \; ; \; T_{11} = \frac{T}{D^3 H}$$

Thus, by using provided data points for (Q_{11}, T_{11}, N_{11}, γ) and by defining the mathematical models $\tilde{Q}_{11}$ and $\tilde{T}_{11}$ as shown in equations (14)-(15), non-linear optimization routines can be used to solve the optimization problems (12)-(13) to get the regression parameters $c \in \mathbb{R}^8$ and $d \in \mathbb{R}^{10}$.

$$\underset{c}{\text{minimize}} \quad \frac{1}{2}\left[Q_{11} - \tilde{Q}_{11}(c, \gamma, N_{11})\right]^2 \tag{12}$$

$$\underset{d}{\text{minimize}} \quad \frac{1}{2}\left[T_{11} - \tilde{T}_{11}(d, \gamma, N_{11})\right]^2 \tag{13}$$

Figs. (13)-(14) show the resulting regression models.

$$\begin{aligned}\tilde{Q}_{11}(c, \gamma, N_{11}) &= c_1\gamma + c_2\gamma^2 + c_3\gamma^3 + \ldots \\ &\quad + c_4\gamma\left[1 - c_5 e^{(c_6 N_{11} + c_7 N_{11}^2 + c_8\gamma)}\right]\end{aligned} \tag{14}$$

$$\begin{aligned}\tilde{T}_{11}(d, \gamma, N_{11}) &= d_1 + d_2\gamma + d_3\gamma^3 + d_4\gamma^5 - \ldots \\ &\quad - d_5 e^{(d_6 N_{11} + d_7 N_{11}^2 + d_8\gamma + d_9\gamma^2 + d_{10}\gamma^3)}\end{aligned} \tag{15}$$

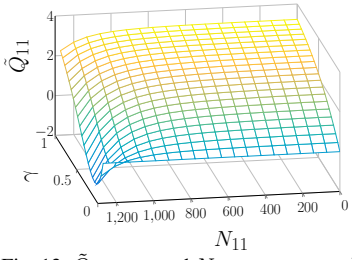

Fig. 13. $\tilde{Q}_{11}$ vs γ and N_{11}

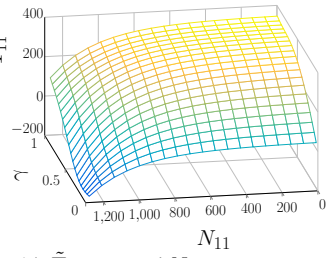

Fig. 14. $\tilde{T}_{11}$ vs γ and N_{11}

Hence, the torque and volumetric flow rate could be computed using equations (14)-(15) and by combining them with the definitions of the unitary variables, we get :

$$Q = \tilde{Q}_{11} D^2 \sqrt{H} \tag{16}$$

$$T = \tilde{T}_{11} D^3 H \tag{17}$$

So, once the pressure head is specified, (14)-(17) could be used to compute Q and T for a given N and γ.

The turbine's efficiency (η) shown in Fig. (15) is given by

$$\eta = \frac{T(\gamma, \omega, H)N}{\rho g H Q(\gamma, \omega, H)} \tag{18}$$

where ρ is the water's density, g is the gravitational acceleration and $\omega = \frac{2\pi N}{60}$.

Consequently, the mechanical power (P_m) shown in figure (16) could be computed by

$$P_m = \eta(\gamma, \omega, H)\rho g H Q(\gamma, \omega, H) \tag{19}$$

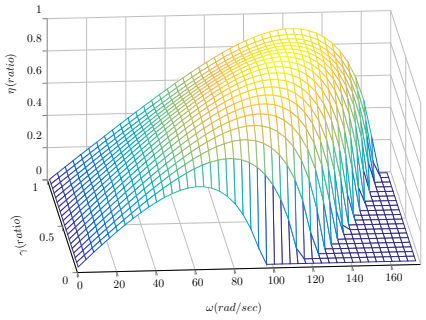

Fig. 15. Efficiency (η) vs ω and γ for $H = 0.35m$ and $D = 0.5m$, where negative efficiency values are set to zero

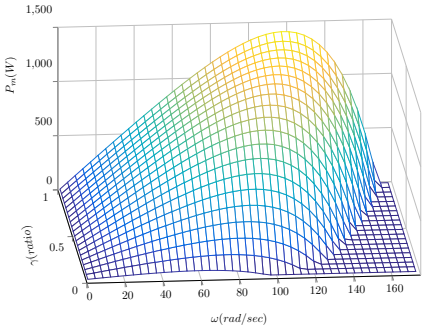

Fig. 16. Mechanical Power (P_m) vs ω and γ for $H = 0.35m$ and $D = 0.5m$, where negative power values are set to zero

This section provides a general philosophy on obtaining the mathematical model for a class of hydraulic turbines with 'Hill Charts' efficiency characteristics. Different definitions of $\tilde{Q}_{11}$ and $\tilde{T}_{11}$ could be used depending on the provided 'Hill Charts'.

2.3.2. *'Hill Chart' scaling*

It is important to note that the 'Hill charts' could be obtained under different operation conditions. In order to scale it to match the requirement of the laboratory benchmark, the diameter of the turbine and the pressure head could be changed to compute Q and T, in addition to re-scaling the resulting regression models to get equations (20)-(21).

$$\tilde{Q}^s_{11}(\gamma, \zeta \times N_{11}) = \alpha \times \tilde{Q}_{11} \tag{20}$$

$$\tilde{T}^s_{11}(\gamma, \zeta \times N_{11}) = \beta \times \tilde{T}_{11} \tag{21}$$

where the scaling coefficients $\alpha, \beta, \zeta > 0$

2.4. *Remarks on modelling approaches*

Compared with simplified linear model [1], look-up table based model [5, 23], and 2-D efficiency models [9, 17], the accuracy of this novel modelling approach is improved, because the chosen regression functions lead to capturing the main patterns in the 'Hill Charts'. Furthermore, the scaling operation makes it flexible to adapt to different experiment environments, the practicability is thus improved. Even the model is less complete than [11, 25], it benefits from lighter computation burden than the dynamic model. This approach could be applied to a class of micro-hydro turbines with 'Hill Chart' efficiency characteristics, which means that it has a wider application range [14]. A comparison of the hydraulic modelling approaches is presented in Table 1.

3. ENERGY CONVERSION CHAINS TOPOLOGIES

3.1. *Topologies review*

A classification of representative power topologies for varible speed Micro-Hydro Power Generation System (MHPGS) is shown in Fig. 17. The topologies are differed from three aspects, namely generators used, mechanical coupling system, and power electronics connection.

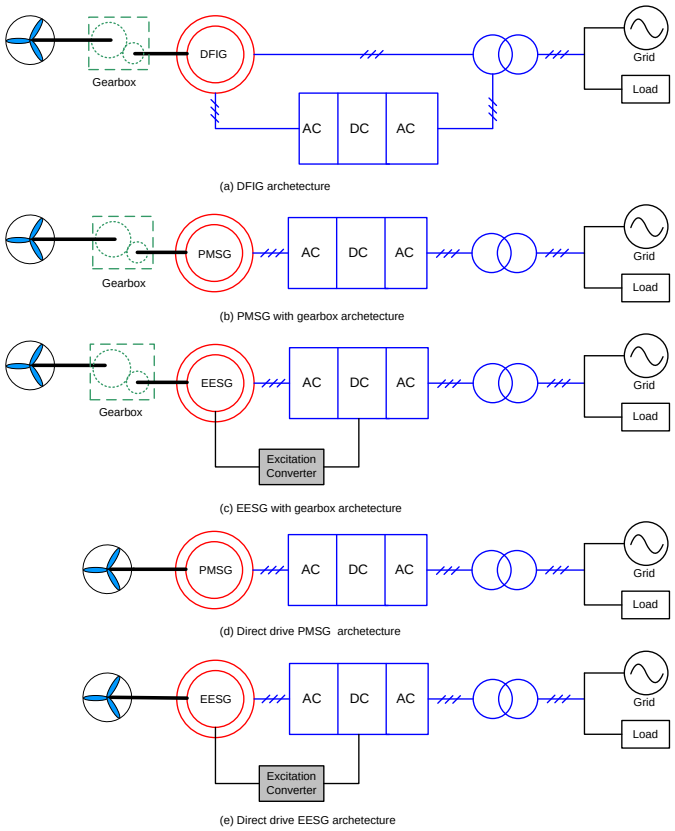

Fig. 17. Available architectures for variable speed MHPGS

A. The generation units can be equipped with either Doubly Feedback Induction Generator (DFIG) [4, 22] or Permanent Magnet Synchronous Generator (PMSG) [2, 14], PMSG can be replaced by Electrically Excitation Synchronous Generator (EESG) [8, 22].
B. Regarding the mechanical connection [8, 22], a gearbox is essentially needed for DFIG. Both the system equipped with gearbox and direct drive system have been used in the PMSG and the EESG.
C. Also, PE connection has great differences for various topologies, DFIG has a direct connection between stator and grid, and a back-to-back Voltage Source Converter (VSC) is connected to rotor and stator [2, 4]. This inverter

Table 1. Comparison of different modelling approaches for Micro-hydro power plants

Model types	Accuracy	Practicality	Less computation burden	Scope of application
Linear torque model	-	+	+++	-
2-D efficiency model	+	++	++	+
Real-time efficiency model	+++	+	-	++
Dynamic hydraulic model	+++	++	- -	++
Previous Regression model	+	+	+	+
'Hill chats' based model	++	++	++	++

The more '+' the better, the more '-' less better.

carries only a fraction of the full scale power by sacrificing the control ability. PMSG has PE units connected to stator and grid, the converter decouples the generator from the grid [14]. An excitation converter is needed for EESG [8].

In terms of their costs and maintenances [2, 4, 8, 22], large maintenances for DFIG are needed for its gearbox and the slip rings, but the costs of induction generator are normally cheaper than PMSG, particular for large capacity. Additionally, direct drive systems now are used widely, as a direct-drive PMSG without gearbox requires less maintenance. While the low rotational speed leads to more pole pairs generator design, resulting in bigger generator volume and higher cost.

3.2. Implemented architecture and its control design

A direct drive PMSG topology is extensively employed in variable speed hydraulic systems for the following reasons [2, 14, 22] : firstly, a PMSG has excellent electric driven capabilities on account of its high efficiency and the high power density; moreover, the converter decouples the generator from the grid, resulting in less effects of grid disturbances; moreover, PMSGs with full power converters have an extended speed regulation range. A variable speed grid-connected MHPGS is shown in Fig. 18. It is composed of a micro-hydraulic turbine such as Propeller, Kaplan, or Bulb, a PMSG, double back-to-back voltage source converters with PWM interacting with the three-phase grid. Some ancillary devices such as the voltage, current, and position sensors are also presented.

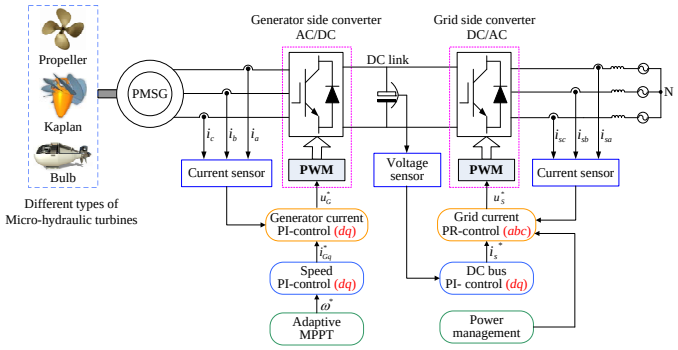

Fig. 18. Architecture of a variable speed MHPGS and its control design [14]

The global control objectives of a variable speed MHPGS involve two aspects : the generator side control and the grid side control [2, 3, 14].

A. Generator side control : its main objective is to achieve the MPPT by controlling the turbine shaft to run at the optimal rotation speed. The speed is determined by the dynamic function of input hydraulic driven torque and the electromagnetic torque of PMSG, which are achieved by current components control. In this paper, an adaptive MPPT technique proposed in [2] is employed. The generator is vector-controlled upon the PMSG Park model. Double PI controllers are applied in both the speed control and current speed control loops [3, 14].

B. Grid side control : it includes double closed control loops, namely, the inner grid current control loop and the outer DC bus voltage loop. DC voltage control ensures the stability of DC bus voltage. The current control achieves high quality current of less harmonics, no distortion, and small frequency vibrations, as well as the power factor to be 1 [14]. In this paper, the PI controller is used to maintain constant DC bus voltage; the grid side current is controlled through three Proportion Resonant (PR) controllers upon the abc three phase frame [3].

4. EXPERIMENTAL RESULTS

4.1. Experiment benchmark

Experiments are conducted in a PHIL experiment benchmark as shown in Fig. 19. The hydraulic turbine is emulated by a real-time physical simulator. The hydraulic mathematical model established in Section 2.3 is achieved in the dSPACE hardware (DS1005). Then, the physical replication of the hydro power operation is achieved by a torque-controlled Direct Current Motor (DCM), the torque tracking control of DCM is implemented into a TMS320F240 digital signal processor. The PMSG is physically coupled to the shaft of DCM, and the generator is connected to the power grid via double back-to-back VSC. The control algorithms of the energy conversion chains are also achieved by the dSPACE modular of DS1005 board, which is built under the Matlab/Simulink environment. The analog measurements and digital variables could be exchanged through the I/O interface [20, 21].

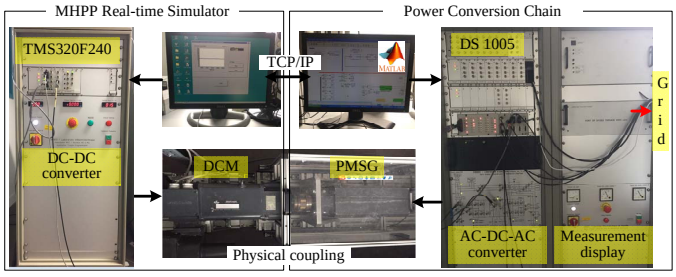

Fig. 19. PHIL experiment benchmark

Parameters of the benchmark used are listed in table 2.

Table 2. Parameters of the experiment benchmark

Parameters	Value	Parameters	Value
Armature R_s	0.17 Ω	Pole pairs	4
d-axis L_q	0.0017 H	Switch frequency	10 kHz
q-axis L_d	0.0019 H	Friction factor	0.01 $N.m.s$
Magnet flux	0.11 Wb	Total inertia	0.03$Kg.m^2$

4.2. *Variable speed control*

To start the hydraulic turbine smoothly, a soft starting process is employed as shown in Fig. 20. Firstly, a small initial torque is added to overcome the friction torque, the speed increases slowly ; Then the controllers start working under no-load state ; Finally, the actuator acts and MPPT mode is enabled, the mechanical power is sent to the generator.

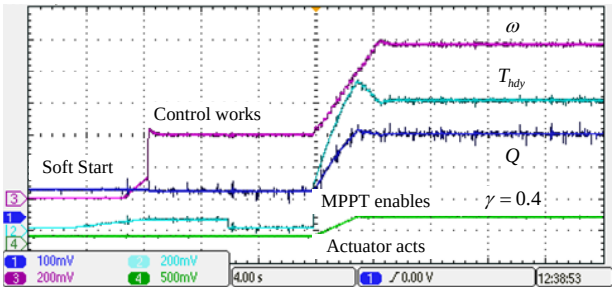

(a) ω $(20rad/s/div)$ the rotation speed, T_{hdy} $(2N.m/div)$ the hydraulic torque, Q $(0.1m^3/s/div)$ the water flow rate, time $(4s/div)$

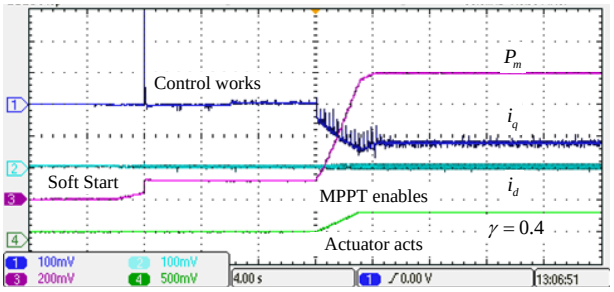

(b) P_m $(200W/div)$ the output mechanical power, i_q $(10A/div)$ the q axis current, i_d $(10A/div)$ the d axis current, time $(4s/div)$
Fig. 20. Starting process of the generator side control

Fig. 21 shows MPPT process with valve opening ratios $\gamma = [0.4, 0.5, 0.4]$. The optimal rotation speed reference is updated by the MPPT, when the valve opening is adjusted. Then, by controlling the q axis current components, the rotation speed could follow the speed reference to maximize the output mechanical power. The d axis current is controlled to be zero.

4.3. *Grid integration control*

Grid integration performance is presented in Fig. 22. In the soft staring process, the DC bus voltage increases smoothly until it reaches the reference value, meanwhile, the hydraulic power is sent to the grid when the valve actuator starts acting as shown in 22a. The active power and reactive power (controlled to be zero) injected to the power grid vary with the guide valve opening in the MPPT process, and DC bus voltage keeps nearly constant as shown in Fig. 22b. Fig. 23 indicates that the injected grid current is well controlled, which works in phase with the grid voltage.

5. CONCLUSIONS

In this paper, numerous modelling approaches of MHPPs are reviewed. An improved modelling approach is presented, which could be applied to a class of micro-hydro turbines with 'Hill Chart' efficiency characteristics. This approach provides preciser 3-D model, and the scaling operation makes it flexible to adapt to different experiment environments. The model benefits from lighter computation burden by sacrificing the non-linear dynamics. A direct drive PMSG architecture is employed in this paper, because its has a wider speed operation range and great anti-disturbance capacity. Experiments results indicates that the variable speed technique can obtain more power from the hydraulic turbine ; the grid side integration is effectively controlled. The hydraulic model established could be used in various hydraulic operating regimes and control study.

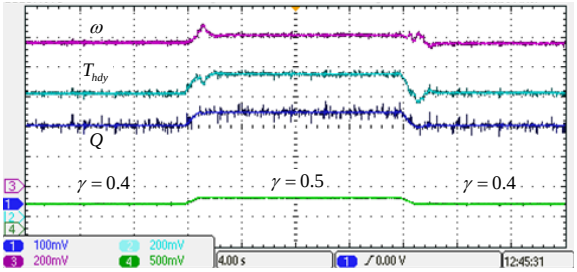

(a) ω $(20rad/s/div)$ the rotation speed, T_{hdy} $(2N.m/div)$ the hydraulic torque reference, Q $(0.1m^3/s/div)$ the water flow rate, time $(4s/div)$

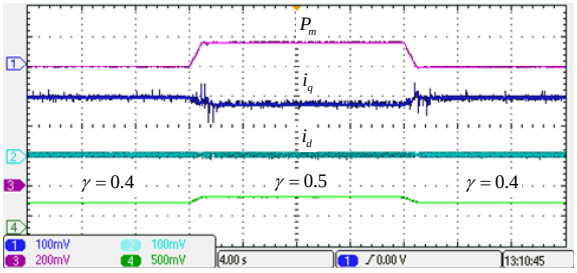

(b) P_m $(200W/div)$ the output mechanical power, i_q $(10A/div)$ the q axis current, i_d $(10A/div)$ the d axis current, time $(4s/div)$
Fig. 21. MPPT process of the generator side control

6. REFERENCE

[1] Aymeric Ansel and Benoit Robyns. Modelling and simulation of an autonomous variable speed micro hydropower station. *Mathematics and computers in simulation*, 71(4-6) :320–332, 2006.

[2] Lakhdar Belhadji, Seddik Bacha, Iulian Munteanu, Axel Rumeau, and Daniel Roye. Adaptive mppt applied to variable-speed microhydropower plant. *IEEE Transactions on Energy Conversion*, 28(1) :34–43, 2013.

[3] Lakhdar Belhadji, Seddik Bacha, and Daniel Roye. Modeling and control of variable-speed micro-hydropower plant based on axial-flow turbine and permanent magnet synchronous generator (mhpp-pmsg). In *IECON 2011-37th Annual Conference on IEEE Industrial Electronics Society*, pages 896–901. IEEE, 2011.

[4] S. Benelghali, M. E. H. Benbouzid, and J. F. Charpentier. Comparison of pmsg and dfig for marine current turbine applications. In *The XIX International Conference on Electrical Machines - ICEM 2010*, pages 1–6, Sept 2010.

[5] Alberto Borghetti, Mauro Di Silvestro, Gleb Naldi, Mario Paolone, and Massimo Alberti. Maximum efficiency point tracking for adjustable-speed small hydro power plant. *16th PSCC, Glasgow, Scotland*, 2008.

[6] Dariusz Borkowski. Laboratory model of small hydropower plant with variable speed operation. *Zeszyty Problemowe–Maszyny Elektryczne*, (3) :100, 2013.

[7] Dariusz Borkowski. Maximum efficiency point tracking (mept) for variable speed small hydropower plant with neural network based estimation of turbine discharge. *IEEE Transactions on Energy Conversion*, 32(3) :1090–1098, 2017.

[8] H. Chen, N. Aït-Ahmed, E. H. Zaïm, and M. Machmoum. Marine tidal current systems : State of the art. In *2012 IEEE International Symposium on Industrial Electronics*, pages 1431–1437, May 2012.

[9] Leon Marcel Oliveira de Mesquita, Jefferson dos Santos Menas, Emanuel Leonardus van Emmenk, and Mauncio Aredes. Maximum power point tracking applied on small hydroelectric power plants. In *Electrical Machines and Systems (ICEMS), 2011 International Conference on*, pages 1–6. IEEE, 2011.

[10] Cesar Farell and John Gulliver. Hydromechanics of variable speed turbines. *Journal of energy engineering*, 113(1) :1–13, 1987.

[11] J. Fraile-Ardanuy, J. I. Perez, I. Sarasua, J. R. Wilhelmi, and J. Fraile-Mora. Speed optimisation module of a hydraulic francis turbine based on

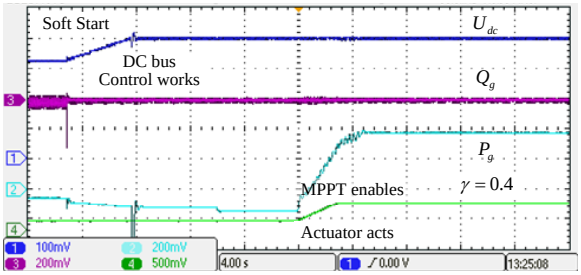

(a) Soft tarting process

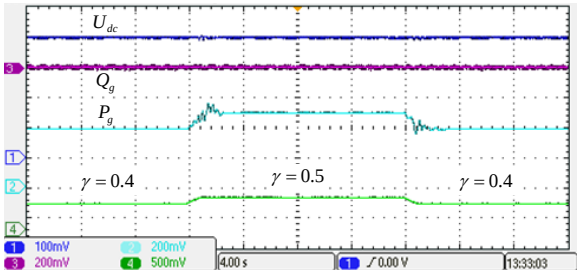

(b) MPPT process

Fig. 22. Grid integration performance, with U_{dc} $(100v/div)$ the DC bus voltage, Q_g $(200var/div)$ the injected reactive power, P_g $(200W/div)$ the injected active power, time $(4s/div)$

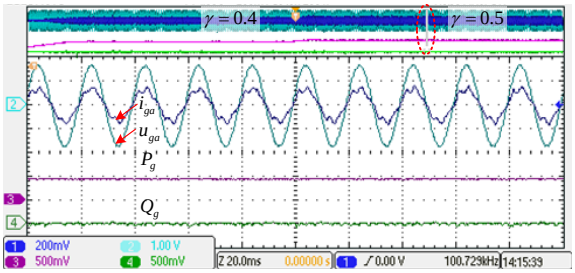

Fig. 23. Grid-injected current, with u_{ga} $(100v/div)$ the grid voltage of phase a, i_{ga} $(2A/div)$ the injected current of phase a, Q_g $(500var/div)$ the reactive power, P_g $(500W/div)$ the active power, time $(4s/div)$

artificial neural networks. application to the dynamic analysis and control of an adjustable speed hydro plant. In *The 2006 IEEE International Joint Conference on Neural Network Proceedings*, pages 4104–4110, 2006.

[12] B. Guo, S. Bacha, M. Alamir, and H. Imanein. An anti-disturbance adrc based mppt for variable speed micro-hydropower plant. In *IECON 2017 - 43rd Annual Conference of the IEEE Industrial Electronics Society*, Oct 2017.

[13] Baoling Guo, Seddik Bacha, and Mazen Alamir. A review on adrc based pmsm control designs. In *IECON 2017*, 2017.

[14] Baoling Guo, Amgad Tarek mohamed, Seddik Bacha, and Mazen S Alamir. Variable speed micro-hydro power plant : modelling, loss analysis, and experiment validation. In *2018 9th International Conference on Information Technology (ICIT)*, Lyon, France, 2018.

[15] Zhuoyu Jiang. Power conversion system for grid connected micro hydro power system with maximum power point tracking, 2017.

[16] Nand Kishor, R.P. Saini, and S.P. Singh. A review on hydropower plant models and control. *Renewable and Sustainable Energy Reviews*, 11(5) :776 – 796, 2007.

[17] JL Marquez, MG Molina, and JM Pacas. Dynamic modeling, simulation and control design of an advanced micro-hydro power plant for distributed generation applications. *International journal of hydrogen energy*, 35(11) :5772–5777, 2010.

[18] Chmn Mello and RJ KOESSLER. Hydraulic turbine and turbine control models for system dynamic studies [j]. *IEEE Transactions on Power Systems*, 7(1) :167–179, 1992.

[19] Hugo Mesnage, Mazen Alamir, Nicolas Perrissin-Fabert, Quentin Alloin, and Seddik Bacha. Hydraulic-turbine start-up with “s-shaped” characteristic. In *Control Conference (ECC), 2015 European*, pages 2328–2333. IEEE, 2015.

[20] Iulian Munteanu, Antoneta Iuliana Bratcu, Maria Andreica, Seddik Bacha, Daniel Roye, and Joel Guiraud. A new method of real-time physical simulation of prime movers used in energy conversion chains. *Simulation Modelling Practice and Theory*, 18(9) :1342–1354, 2010.

[21] Iulian Munteanu, Antoneta Iuliana Bratcu, Seddik Bacha, Daniel Roye, and Joël Guiraud. Hardware-in-the-loop-based simulator for a class of variable-speed wind energy conversion systems : Design and performance assessment. *IEEE Transactions on Energy Conversion*, 25(2) :564–576, 2010.

[22] Sabar Nababan, E Muljadi, and Frede Blaabjerg. An overview of power topologies for micro-hydro turbines. In *Power Electronics for Distributed Generation Systems (PEDG), 2012 3rd IEEE International Symposium on*, pages 737–744. IEEE, 2012.

[23] Juan I Perez-Diaz and Jesús Fraile-Ardanuy. Neural networks for optimal operation of a run-of-river adjustable speed hydro power plant with axial-flow propeller turbine. In *Control and Automation, 2008 16th Mediterranean Conference on*, pages 309–314. IEEE, 2008.

[24] Joachim RAABE. Hydro power the design, use and function of hydromechanical, hydraulic and electrical equipment. page 684 p. : ill. ; 25 cm, 1985.

[25] O. H. Souza, N. Barbieri, and A. H. M. Santos. Study of hydraulic transients in hydropower plants through simulation of nonlinear model of penstock and hydraulic turbine model. *IEEE Transactions on Power Systems*, 14(4) :1269–1272, Nov 1999.

[26] A. Tessarolo, F. Luise, P. Raffin, and M. Degano. Traditional hydropower plant revamping based on a variable-speed surface permanent-magnet high-torque-density generator. In *2011 International Conference on Clean Electrical Power (ICCEP)*, pages 350–356, June 2011.

[27] M. A. Vallet, S. Bacha, I. Munteanu, A. I. Bratcu, and D. Roye. Management and control of operating regimes of cross-flow water turbines. *IEEE Transactions on Industrial Electronics*, 58(5) :1866–1876, May 2011.

[28] Omkar Yadav, Nand Kishor, Jesus Fraile-Ardanuy, Soumya R Mohanty, Juan I Pérez, and José I Sarasúa. Pond head level control in a run-of-river hydro power plant using fuzzy controller. In *Intelligent System Application to Power Systems (ISAP), 2011 16th International Conference on*, pages 1–5. IEEE, 2011.